polymers

MDPI

Article

A Design-Oriented Combined Model (7 MPa to 190 MPa) for FRP-Confined Circular Short Columns

Zehra Canan Girgin [1,*] and Konuralp Girgin [2]

Received: 3 August 2015 ; Accepted: 21 September 2015 ; Published: 28 September 2015
Academic Editors: Alper Ilki and Masoud Motavalli

[1] Structural Systems Division, Architecture Faculty, Yildiz Technical University, Istanbul 34349, Turkey
[2] Civil Engineering Faculty, Istanbul Technical University, Istanbul 34469, Turkey; girgink@itu.edu.tr
* Correspondence: zcgirgin@yildiz.edu.tr; Tel.: +90-212-383-2616; Fax: +90-212-383-2650

Abstract: This study addresses a design oriented combined model to predict the ultimate strengths and ultimate strains in an extensive range of unconfined strength (7 to 190 MPa) for the axially loaded fiber-reinforced polymer (FRP)-wrapped circular short columns. Modified Hoek-Brown strength criterion, which was previously extended to FRP-confined concrete from 7 to 108 MPa, is revisited and verified. An empirical strength model beyond 108 MPa encompassing ultra-high strength concrete (UHSC) and ultra-high performance concrete (UHPC) data, as well as empirical strain models, are defined to accomplish the design oriented combined model. This article especially focuses on the verification of the proposed strain models. The assessment performances of those models for carbon FRP (CFRP) and glass FRP (GFRP) confinement are compared with specific models in the current literature. Strength and strain predictions for UHSC and UHPC are integrated into the design oriented combined model as well. The assessments on this model agree with the experimental results in high accuracy.

Keywords: confined concrete; FRP; strength; strain; design oriented model; Hoek-Brown; UHSC; UHPC

1. Introduction

FRP composites have been used in the construction sector for over two decades due to their properties, such as high strength-to-weight ratio, high tensile strength and modulus, corrosion resistance, and durability. FRP confinement through a glass-fiber tube [1–3], frequently using carbon [4–10], sometimes aramid [11,12], and recently basalt [13], recycled plastic [12,14,15], and natural [16] fiber sheets were used in the experimental studies so far. In addition, the confinement with polypropylene ropes [17,18], FRP+steel tube [19], or prestressing at several levels [20] are recent material types and methods.

The experimental studies are often in the cylinder strength range of f_{co} = 20–50 MPa [1,4–6,10]. Low strength data, under 20 MPa [4,5,8,21], and ultra-high strength concrete (UHSC) or ultra-high performance concrete (UHPC) data, over 100 MPa [22–26], are limited compared with the normal strength range (20 to 50 MPa). Increasing compressive strength levels in the construction sector enables to reduce member sizes. Higher confining pressure through an FRP jacket is required to prevent the inherent brittle behavior in UHSC or UHPC.

The Hoek-Brown criterion [27] enables to predict the tensile stresses in the compression-tension region contrary to the Mohr–Coulomb criterion. The Hoek-Brown criterion was initially extended and modified to actively confined concrete [28] and then to FRP-confined concrete [29]. The modified strength criterion for FRP confinement [29] was verified with the data from f_{co} = 7 to 108 MPa.

However, the data beyond 108 MPa was very limited to calibrate this model. In this study, a modified Hoek–Brown strength criterion is revisited exactly to define, especially, the upper strength ranges. The database was also updated (7 to 190 MPa) with new data covering UHSC and UHPC from the current literature. To complete the combined design oriented model, empirical and practical models with high accuracy are proposed for ultimate strengths and strains.

2. Strength and Strain Models for FRP Confinement

2.1. Confinement with FRP

Under triaxial compressive stresses, the columns are subjected to major compressive stresses (σ_1) along the axial axis of the column and minor principal stresses (σ_3, f_l) enhancing the unconfined compressive strength of concrete (σ_c, f_{co}) (Figure 1). Lateral passive confining pressure (f_l) can be presently provided by FRP confinement (sheets and tubes) instead of steel confinement as well. f_l can be expressed in terms of the ultimate fiber strain (ε_{fu}) and lateral modulus (E_l) of the FRP jacket:

$$f_l = \sigma_3 = E_l \, \varepsilon_{fu} \tag{1}$$

where:

$$E_l = \frac{2 E_f \, t}{D} \tag{2}$$

or in terms of hoop tensile strength of FRP (σ_{frp} or f_{frp}):

$$f_l = \frac{2 \sigma_{frp} \, t}{D} \tag{3}$$

thus:

$$f_l = \frac{2 E_f \, \varepsilon_{fu} \, t}{D} = \frac{1}{2} \rho_f E_f \, \varepsilon_{fu}, \; \rho_f = \frac{4t}{D} \tag{4}$$

where D, E_f, ρ_f, and t denote the diameter of concrete core, Young's modulus, volumetric ratio, and thickness of FRP jacket, respectively.

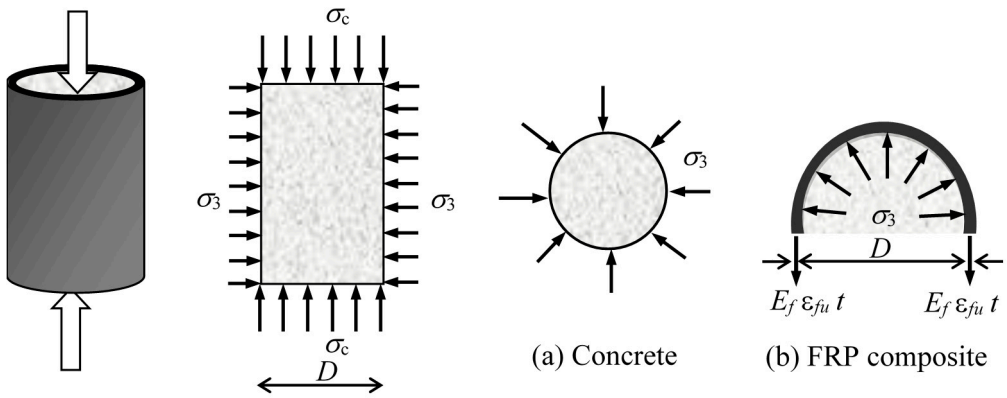

Figure 1. Development of confining pressure in FRP confined concrete. (**a**) Confining pressure to concrete; (**b**) Ultimate confining pressure by FRP composite on concrete.

FRP fiber strain (ε_{fu}) is generally based on coupon or manufacturer data, and is often smaller than actual hoop rupture strain ($\varepsilon_{h,u}$). While the relationships generally take coupon or manufacturer data into consideration, a few relationships [30–32] were also proposed in terms of actual confinement pressure ($f_{l,a}$) and actual confinement ratio ($f_{l,a}/f_{co}$) through the hoop rupture strain ($\varepsilon_{h,u}$):

$$\varepsilon_{h,u} = k_{\varepsilon,f} \varepsilon_{fu} \tag{5}$$

$$f_{l,a} = \frac{2E_f \varepsilon_{h,u}\, t}{D} \tag{6}$$

where $k_{\varepsilon,f}$ signifies the strain reduction factor [33,34] smaller than one. In the literature, the average values of $k_{\varepsilon,f}$ were determined to be 0.680, 0.793, 0.732 for CFRP, GFRP, and AFRP sheets, respectively [32]. It was realized that $k_{\varepsilon,f}$ decreases as the unconfined compressive strength level increases, *i.e.*, $k_{\varepsilon,f}$ is 0.737, 0.656, 0.548 in normal, high, and ultra-high strength concrete confined with CFRP wraps, respectively [35]. Herein, it is noted that, to propose a relationship based on $\varepsilon_{h,u}$ instead of ε_{fu} may be realistic, but it may not be proper for the practical assessment of ultimate strength.

In the literature, several strength models are available, however, the design oriented models predicting both stress and strain are more limited. Specific models to assess the ultimate strengths and strains in circular short columns are given in Table 1. It is mentioned that while f_l/f_{co} is higher than 0.07, f_{cc} signifies the ultimate strength, otherwise denotes as the peak strength.

Stresses and strains will be verified through Integral Absolute Error (IAE), which was defined previously [28,29], and relative error or Average Absolute Error (AAE) in which:

$$\text{IAE}\ (\%) = \sum \frac{|o_i - p_i|}{\sum o_i} \times 100,\ \text{AAE}\ (\%) = \frac{\sum |(o_i - p_i)/o_i| \times 100}{n},\ (o_i = \text{observed},\ p_i = \text{predicted}) \tag{7}$$

Table 1. Strength and strain models in circular sections.

Source	Strength Model	Strain Model
Fardis and Khalili [2] strength model based on Richart *et al.* [36] (f_{co} = 20–50 MPa)	$\frac{f_{cc}}{f_{co}} = 1 + 4.1\frac{f_l}{f_{co}}$	$\varepsilon_{cu} = \varepsilon_{co} + 0.0005\frac{E_l}{f_{co}}$
Mander *et al.* [37] Saadatmanesh *et al.* [38]	$\frac{f_{cc}}{f_{co}} = 2.254\sqrt{1 + 7.94\frac{f_l}{f_{co}}} - 2\frac{f_l}{f_{co}} - 1.254$	$\frac{\varepsilon_{cu}}{\varepsilon_{co}} = 1 + 5\left(\frac{f_{cc}}{f_{co}} - 1\right)$
ACI 440 [39]		$\varepsilon_{cu} = \frac{1.71\,(5f_{cc} - 4f_{co})}{E_{co}}$
Karbhari and Gao [5] (f_{co} = 38 MPa)	$\frac{f_{cc}}{f_{co}} = 1 + 2.1\left(\frac{f_l}{f_{co}}\right)^{0.87}$ Model II	$\varepsilon_{cu} = \varepsilon_{co} + 0.01\frac{f_l}{f_{co}}$
Kono *et al.* [40] (f_{co} = 32–35 MPa)	$\frac{f_{cc}}{f_{co}} = 1 + 0.0572\, f_l$	$\frac{\varepsilon_{cu}}{\varepsilon_{co}} = 1 + 0.28 f_l$
Saafi *et al.* [41] (f_{co} = 38 MPa)	$\frac{f_{cc}}{f_{co}} = 1 + 2.2\left(\frac{f_l}{f_{co}}\right)^{0.84}$	$\frac{\varepsilon_{cu}}{\varepsilon_{co}} = 1 + \left(537\varepsilon_{fu} + 2.6\right)\left(\frac{f_{cc}}{f_{co}} - 1\right)$
Spoelstra and Monti [33] (f_{co} = 30–50 MPa)	$\frac{f_{cc}}{f_{co}} = 0.2 + 3\left(\frac{f_l}{f_{co}}\right)^{0.5}$	$\frac{\varepsilon_{cu}}{\varepsilon_{co}} = 2 + 1.25\frac{E_{co}}{f_{co}}\varepsilon_{fu}\left(\frac{f_l}{f_{co}}\right)^{0.5}$ [a]
Xiao and Wu [42] (f_{co} = 34–55 MPa, CFRP)	$\frac{f_{cc}}{f_{co}} = 1.1 + \left[4.1 - 0.75\left(f_{co}^2/E_l\right)\right]\frac{f_l}{f_{co}}$	$\varepsilon_{cu} = \frac{\varepsilon_{fu} - 0.0005}{7(f_{co}/E_l)^{0.8}}$
Toutanji-modified [43] (f_{co} = 31 MPa)	$\frac{f_{cc}}{f_{co}} = 1 + 2.3\left(\frac{f_l}{f_{co}}\right)^{0.85}$	$\frac{\varepsilon_{cu}}{\varepsilon_{co}} = 1 + \left(310.57\varepsilon_{fu} + 1.9\right)\left(\frac{f_{cc}}{f_{co}} - 1\right)$
Lam and Teng [30] (f_{co} = 27–55 MPa)	$\frac{f_{cc}}{f_{co}} = 1 + 3.3\frac{f_{l,a}}{f_{co}}\ \left(\frac{f_{l,a}}{f_{co}} \geqslant 0.07\right)$	$\frac{\varepsilon_{cu}}{\varepsilon_{co}} = 1.75 + 12\left(\frac{f_{l,a}}{f_{co}}\right)\left(\frac{\varepsilon_{h,u}}{\varepsilon_{co}}\right)^{0.45}$ $\frac{\varepsilon_{cu}}{\varepsilon_{co}} = 1.92 + 24.45\frac{f_{l,a}}{f_{co}}\ (CFRP)$ $\frac{\varepsilon_{cu}}{\varepsilon_{co}} = 1.75 + 5.53\left(\frac{f_l}{f_{co}}\right)\left(\frac{\varepsilon_{fu}}{\varepsilon_{co}}\right)^{0.45}\ (CFRP)$
Teng *et al.* [44] (f_{co} = 38–46 MPa)	$\frac{f_{cc}}{f_{co}} = 1 + 3.5\,(\rho_k - 0.01)\,\rho_\varepsilon\ (\rho_k \geqslant 0.01)$ $\rho_k = \frac{2E_f t\,\varepsilon_{co}}{D\,f_{co}}, \rho_\varepsilon = \frac{0.586\,\varepsilon_{fu}}{\varepsilon_{co}}$	$\frac{\varepsilon_{cu}}{\varepsilon_{co}} = 1.75 + 6.5\,\rho_k^{0.8}\rho_\varepsilon^{1.45}$
Benzaid *et al.* [31] (f_{co} = 29–62 MPa, CFRP)	$\frac{f_{cc}}{f_{co}} = 1 + 1.6\frac{f_l}{f_{co}},\ \frac{f_{cc}}{f_{co}} = 1 + 2.2\frac{f_{l,a}}{f_{co}}$	$\frac{\varepsilon_{cu}}{\varepsilon_{co}} = 2 + 5.5\frac{f_l}{f_{co}},\ \frac{\varepsilon_{cu}}{\varepsilon_{co}} = 2 + 7.6\frac{f_{l,a}}{f_{co}}$
Rousakis *et al.* [45,46] (f_{co} = 9–170 MPa)	$\frac{f_{cc}}{f_{co}} = 1 + \left(\frac{\rho_f E_f}{f_{co}}\right)\left(\frac{\alpha E_f 10^{-6}}{E_{f\mu}} + \beta\right)$ [b]	$\frac{\varepsilon_{cu}}{\varepsilon_{co}} = 1 + 24.8\frac{4E_f t}{D f_{co}}\left(\frac{-0.45E_f 10^{-6}}{E_{f\mu}} + 0.0223\right)\left(\frac{40E_f t}{E_{f\mu} D}\right)^{-0.16}$
Ozbakkaloglu and Lim [32]	$\frac{f_{cc}}{f_{co}} = 1 + 3.64\frac{f_{l,a}}{f_{co}}\ (CFRP)$	$\frac{\varepsilon_{cu}}{\varepsilon_{co}} = 2 + 17.41\frac{f_{l,a}}{f_{co}}\ (CFRP)$
	$\frac{f_{cc}}{f_{co}} = 1 + 2.64\frac{f_{l,a}}{f_{co}}\ (GFRP)$	$\frac{\varepsilon_{cu}}{\varepsilon_{co}} = 2 + 24.47\frac{f_{l,a}}{f_{co}}\ (GFRP)$

[a] This model is focused in the Section 3.2; [b] $E_{f\mu}$ = 10 MPa (for units compliance); $\alpha = -0.336$, $\beta = 0.0223$ for FRP sheets ; $\alpha = -0.23$, $\beta = 0.0195$ for FRP tube.

2.2. Strength Models

Earlier models for FRP confinement (Table 1) were proposed based on steel-confined concrete [2,36–38]. Most models [32,33,41,43] for steel and FRP-confined concrete are based on the Mohr–Coulomb criterion after Richart *et al.*'s pioneering investigation [36].

Hoek-Brown [27] and Johnston [47] strength criteria from rock mechanics were extended and modified [29,48] to precisely predict f_{cc} in FRP-confined short columns from f_{co} = 7 to 108 MPa. Data concerning different sheet types (Carbon, glass, aramid fiber, *etc.*) and GFRP tube (length-to-diameter ratio is about 2, low to high confinement ratios up to 2.0) were taken into consideration in two modified criteria (Table 2).

Table 2. Modified strength models from rock mechanics.

Reference	Failure Criterion for Rock	Modified Form for FRP Confined Concrete
Girgin [29]	Hoek-Brown *et al.* [27] $\sigma_1 = \sigma_3 + \sigma_c \left(m \frac{\sigma_3}{\sigma_c} + s \right)^{0.5}$ $\sigma_c \geqslant 20$ MPa	$f_{cc} = f_l + \left(s f_{co}^2 + m f_{co} f_l \right)^{1/2}$ s = 1 for intact rock or undamaged concrete m = 2.9 (f_{co} = 7 to18 MPa) m = 6.34−0.076 f_{co} (f_{co} = 20 to 82 MPa) m = 0.1 (f_{co} = 82 to 108 MPa)
Girgin [48]	Johnston [47] $\frac{\sigma_1}{\sigma_c} = \left(1 + \frac{M}{B} . \frac{\sigma_3}{\sigma_c} \right)^B$	$\frac{f_{cc}}{f_{co}} = \left(1 + \frac{M}{B} . \frac{f_l}{f_{co}} \right)^B$ $B = 1 - 0.0172 \ (\log f_{co})^2$, f_{co} in kPa $M = 0.0035 f_{co}^2 - 0.056 f_{co} + 2.83$ (f_{co} = 7 to 24 MPa) $M = 0.0003 f_{co}^2 - 0.076 f_{co} + 5.46$ (f_{co} = 25 to 108 MPa)

In this study, we hope to re-verify m coefficients of modified Hoek-Brown criterion and to also address higher compressive strength levels (f_{co} > 108 MPa). The current database [1,4–8,11,12,21–23,41,42,49–63] composed of n = 198 averaged data was updated with n = 40 data [9,10,22–26,35,64] from the recent literature on HSC, UHSC, and UHPC for the FRP sheet types mentioned above. Meanwhile, UHSC and UHPC strength data in the literature are available up to 113.6 and 188 MPa, respectively.

2.3. Strain Models

The ultimate strain of confined concrete (ε_{cu}) is generally defined in terms of confining pressure, confinement ratio, strengthening ratio, and some additional parameters such as ultimate strain of FRP, initial elastic modulus and confinement modulus (f_l, f_l/f_{co}, $f_{l,a}/f_{co}$, f_{cc}/f_{co}, ε_f, E_{co}, E_l).

ACI 440 [39], and Spoelstra and Monti [33] used the initial elastic modulus of concrete (E_{co}) in the suggested models (Table 1). Several formulas [65–71] to predict E_{co} were proposed in the current literature so far. Herein, *fib* MC2010 [70] was used in the assessment of these models. That model gives similar results to Noguchi *et al.*'s [69] model, which was performed for more than 3000 tests, for the limestone aggregates commonly used in concrete. Although *fib* MC2010 [70] model was originally defined up to 80 MPa, the model also matches with the test results of UHSC and UHPC [71] from 107 to 179 MPa. Thus, the model in Equation (8) was used from 20 to 190 MPa.

$$E_{co} = 21500 \sqrt[3]{\frac{f_{co}}{10}} \tag{8}$$

Strain models are often expressed in terms of strain enhancement ($\varepsilon_{cu}/\varepsilon_{co}$) or ductility. However, ε_{co} values are not always determined experimentally, and can usually be assumed to be 0.002 [5,10,32,42] or calculated according to some empirical relationships in the current literature. In this study, ε_{co} values were derived as per the following formula in Eurocode 2 [72]:

$$\varepsilon_{co} = \frac{0.7}{1000} f_{co}^{0.31} \tag{9}$$

Hoek-Brown failure criterion from rock mechanics [27] is a strength model. For this reason, in this study, combining strain models will be introduced for the most common types of FRP confinement. Thus, the database was mainly compiled with the experimental results of CFRP-wrapped specimens (n = 177) and more limited data of GFRP-wrapped specimens (n = 62). Meanwhile, higher scattering in ultimate strain data (ε_{cu}) is generally observed compared with those of ultimate strengths (f_{cc}), and less data for strains are available in the current literature. Lower and upper limits of strength and strain data are not exactly the same due to some absent strain data. The lower limits of available strain data correspond to f_{co} = 15 MPa (CFRP) and 18 MPa (GFRP). The upper limit of strength data is f_{co} = 188 MPa. There are discontinuities (from 50 to 80 MPa) in the strength ranges of limited GFRP-wrapped specimens.

3. Results and Discussion

In this study, a design-oriented combined model is proposed to predict the ultimate strengths (f_{cc}) and ultimate strains (ε_{cu}) in the axially loaded FRP-confined circular short columns. The upper limit (f_{co} = 108 MPa) of the modified Hoek–Brown strength criterion [29] is revisited and verified. An empirical strength model encompassing UHSC and UHPC data up to f_{co} = 190 MPa, as well as empirical strain models, are defined to accomplish the design-oriented combined model.

3.1. Ultimate Strength Prediction

In two previous studies [29,48], the performances of the specific strength models in the current literature were compared with the presented modified Hoek–Brown and Johnston strength criteria. These comparisons were conducted through IAE and AAE ratios with respect to the concerning strength ranges.

It was concluded that the strength models [2,36–38] based on steel confinement give rise to higher estimation than experimental ones in each relevant strength range known in the current literature [1,5,33,73]. While the prediction performance of some models are restricted concerning range [22], some of those models are also capable of reasonably predicting wider data ranges [5,33,41]. Specific strength models generally overestimate the ultimate strengths (f_{cc}) for f_{co} > 70 MPa [1,5,22,33,41,43,44,50,55] or for f_{co} < 20 MPa [1,22,44], however, some models having a good accuracy for all the data ranges are also available [45]. Herein, the performance details of those strength models will not be mentioned again in detail.

IAE and AAE ratios of the proposed modified Hoek-Brown strength criterion [29], as well as modified Johnston strength criterion [48], are under 6% for each specific strength range. It should be mentioned that the prediction performance based on the ranges of cylinder strength (f_{co}) may be more meaningful than the one error ratio (*i.e.*, AAE, *etc.*) often used in the current literature.

In this study, the expressions of m coefficient (Table 2) in the modified Hoek–Brown strength criterion were not changed, m = 0.1 is valid from f_{co} = 82 to 114 MPa according to the comparisons in this study (Figure 2a). However, for compressive strength levels over 114 MPa, only the m coefficient may not be sufficient for very satisfactory estimations; therefore, the following empirical relationship from f_{co} = 108 to 190 MPa for f_l/f_{co} = 0 to 1.6 is asserted to assess the ultimate strength of circular short columns strengthened with CFRP, GFRP, and AFRP jackets:

$$f_{cc} = 160\frac{f_l}{f_{co}} + 108 \ (n = 31,\ R = 0.982,\ \text{IAE} = 5.5\%,\ \text{AAE} = 5.7\%) \tag{10}$$

Equation (10) addresses UHSC data, as well as UHPC data [9,22–26,35], with high accuracy (Figure 2b).

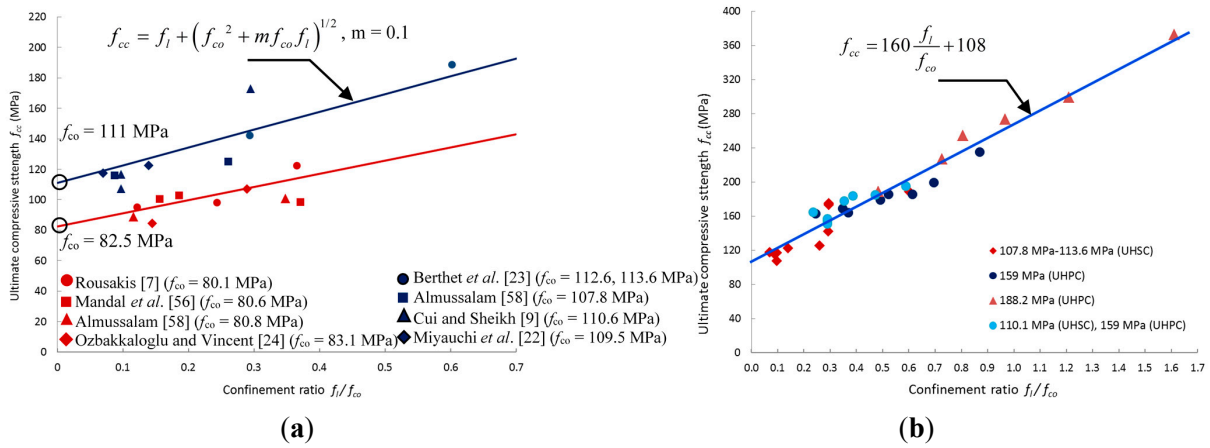

Figure 2. (**a**) Verification of modified Hoek–Brown criterion for high and ultra-high compressive strength levels; (**b**) Proposed empirical model from f_{co} = 108 to 190 MPa for UHSC and UHPC data of CFRP, GFRP, AFRP jackets.

3.2. Ultimate Strain Prediction

The prediction capabilities of specific strain models [2,32,33,38–41,43,44,46,73] are investigated. Following this assessment, the empirical models of this study are introduced to predict the ultimate strains (ε_{cu}) with high accuracy. Meanwhile, strain values deviating significantly from the general trend were discarded from the analyses.

Figure 3 illustrates the performance charts of those specific strain models, via IAE and AAE ratios for CFRP and GFRP confinement. 45-degree line passing through the origin represents the perfect predictions of strains in the charts. The lower and upper parts of this line indicate conservative and unconservative strain estimations, respectively. The specific models [2,32,33,38–41,43,44,46,73] were investigated with regard to the range of database in this study. However, it should be mentioned that those models tend to significantly overestimate the strain capacity, at or over about f_{co} = 100 MPa. Thus, the upper value of strain data was limited to f_{co} = 110 MPa, except for the asserted strain models of this study. The models developed in this study reflect all the database.

Strain models by ACI 440 [39], and Spoelstra and Monti [33] contain the concrete initial elastic modulus (E_{co}). This parameter was defined in Equation (8). In the models based on ε_{cu} [2,5,39,42], those strains were converted to $\varepsilon_{cu}/\varepsilon_{co}$ ratios, as per Equation (9). As seen from Figure 3, the earlier models, such as ACI 440 [39] and those of Saadatmanesh *et al.* [38] underestimate the strain enhancement ($\varepsilon_{cu}/\varepsilon_{co}$) due to FRP confinement, especially for GFRP-wrapped specimens. As f_{co} increases, conservative predictions in Kono *et al.*'s model [40] lead to unsafe results in high confinement levels. Fardis and Khalili's model [2] overestimates the strain enhancement for CFRP jackets, and underestimates those of GFRP jackets. The models by Saafi *et al.* [41], and De Lorenzis and Tepfers [73] are, respectively, characterized with a considerable overestimation and a substantial underestimation, increasing with the confinement ratio of CFRP and GFRP sheets. Toutanji's model [43], compared to similar models, implies relatively proper values. If Spoelstra and Monti's [33] model is implemented via actual confinement values ($\varepsilon_{h,u}, f_{l,a}$) regarding [74], the model reveals sensitive predictions instead of significant overestimations for CFRP sheets. The evaluation results for two cases under consideration are also displayed in Figure 3. It should be mentioned that the model was referred to on the basis of ε_{fu}, f_l in the previous studies [75].

This study also signifies an important point arising from error definitions, *i.e.*, Integral Absolute Error (IAE) may be more sensitive than common Average Absolute Error (AAE). In AAE definitions, the difference between observed and predicted value is small for lower strength or strain values, otherwise the differences between higher values are also high. This case may reflect more unreliable verification results. Otherwise, as for IAE, the error definition based on the ratio of strength or strain

differences may lead to a more accurate evaluation, by surpassing the differences due to lower or extreme values. The difference between AAE and IAE ratios may also be realized from Figure 3.

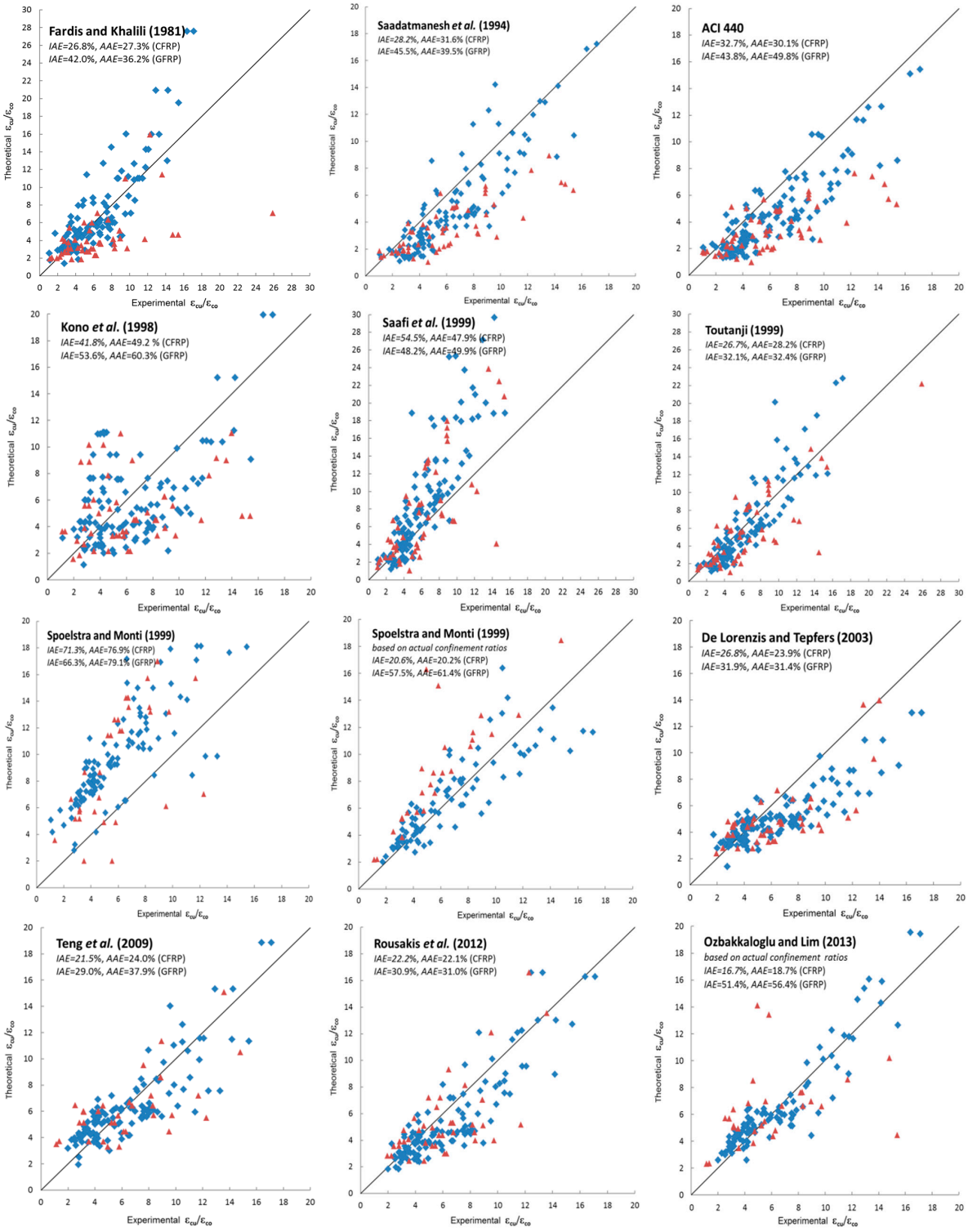

Figure 3. Accuracy of strain models in the current literature columns confined with CFRP and GFRP wraps (f_{co} from 15 to 110 MPa, ♦ for CFRP sheets, ▲ for GFRP sheets).

The strain models of this study were expressed and verified in detail (Table 3). These models were categorized in two groups (CFRP, GFRP) in terms of confinement ratios (f_l/f_{co}, $f_{l,a}/f_{co}$), as per

unconfined strength (f_{co}) ranges, to provide practical assessments. f_{co} does not significantly affect the form of curve; however, two compressive strength levels (e.g., about 50 and 100 MPa for CFRP sheets) are realized from different data distributions. The definition range and curve of any model were achieved by taking this dissimilarity into consideration. Available UHSC and UHPC data are characterized through a linear form within the range of confinement ratio. Any relationship beyond f_{co} = 170 MPa was not described due to the fact that there was only available one data set [25] and a continuously lowering slope. On the other hand, the strain model for actual confinement ratios ($f_{l,a}/f_{co}$) was attained in a wide range, from low strength up to about 100 MPa; however, ε_{cu} data is very limited beyond this.

Strain enhancements ($\varepsilon_{cu}/\varepsilon_{co}$) via these strain models may be assessed with high precision (Figure 4). The prediction performances of specific models (Table 1) and introduced strain models are compared in Figure 5.

Table 3. The strain models developed in this study and prediction capacity.

Parameter		Strain Models	Range of Data	*n*	IAE %	AAE %	Figures
Models for CFRP sheets							
f_l/f_{co}	Ia	$\frac{\varepsilon_{cu}}{\varepsilon_{co}} = -2.77\left(\frac{f_l}{f_{co}}\right)^2 + 12.67\left(\frac{f_l}{f_{co}}\right) - 0.061 f_{co} + 5.07$	15 MPa $\leqslant f_{co} \leqslant$ 50 MPa [a] 0.11 $\leqslant f_l/f_{co} \leqslant$ 1.78	102	13.3	13.5	-
	Ib	$\frac{\varepsilon_{cu}}{\varepsilon_{co}} = -4.24\left(\frac{f_l}{f_{co}}\right)^2 + 15.4\left(\frac{f_l}{f_{co}}\right) + 2.23$	15 MPa $\leqslant f_{co} \leqslant$ 50 MPa 0.11 $\leqslant f_l/f_{co} \leqslant$ 1.78	102	12.6	13.1	Figure 4a
	II	$\frac{\varepsilon_{cu}}{\varepsilon_{co}} = -2.62\left(\frac{f_l}{f_{co}}\right)^2 + 10.94\left(\frac{f_l}{f_{co}}\right) + 1.0$	50 MPa $< f_{co} \leqslant$ 103 MPa 0.12 $\leqslant f_l/f_{co} \leqslant$ 0.58	45	11.7	11.0	
	III	$\frac{\varepsilon_{cu}}{\varepsilon_{co}} = 0.57\left(\frac{f_l}{f_{co}}\right) + 1.0$	109 MPa $< f_{co} \leqslant$ 170 MPa [b] 0.07 $\leqslant f_l/f_{co} \leqslant$ 0.87	10	5.7	6.2	
$f_{l,a}/f_{co}$	IV	$\frac{\varepsilon_{cu}}{\varepsilon_{co}} = -6\left(\frac{f_{l,a}}{f_{co}}\right)^2 + 20.15\left(\frac{f_{l,a}}{f_{co}}\right) - 0.032 f_{co} + 3.5$	20 MPa $< f_{co} \leqslant$ 103 MPa 0.03 $\leqslant f_{l,a}/f_{co} \leqslant$ 1.01	96	8.6	9.7	Figure 4b
Models for GFRP sheets							
f_l/f_{co}	V	$\frac{\varepsilon_{cu}}{\varepsilon_{co}} = -1.85\left(\frac{f_l}{f_{co}}\right)^2 + 8.62\left(\frac{f_l}{f_{co}}\right) + 4.4$	18 MPa $\leqslant f_{co} \leqslant$ 50 MPa 0.09 $\leqslant f_l/f_{co} \leqslant$ 2.0	33	13.4	12.3	Figure 4a
	VI	$\frac{\varepsilon_{cu}}{\varepsilon_{co}} = -6.4\left(\frac{f_l}{f_{co}}\right)^2 + 12.43\left(\frac{f_l}{f_{co}}\right) + 0.9$	80 MPa $< f_{co} \leqslant$ 159 MPa 0.1 $\leqslant f_l/f_{co} \leqslant$ 0.6	10	11.9	12.3	
$f_{l,a}/f_{co}$	VII	$\frac{\varepsilon_{cu}}{\varepsilon_{co}} = -2.03\left(\frac{f_{l,a}}{f_{co}}\right)^2 + 10.41\left(\frac{f_{l,a}}{f_{co}}\right) + 1.41$	18 MPa $\leqslant f_{co} \leqslant$ 111 MPa 0.013 $\leqslant f_{l,a}/f_{co} \leqslant$ 1.958	13	5.8	8.8	Figure 4b

[a] The model is also valid up to f_{co} = 85 MPa and f_l/f_{co} = 0.4 with 19.2% IAE and 21.0% AAE for 50–85 MPa range; [b] UHPC data was also included.

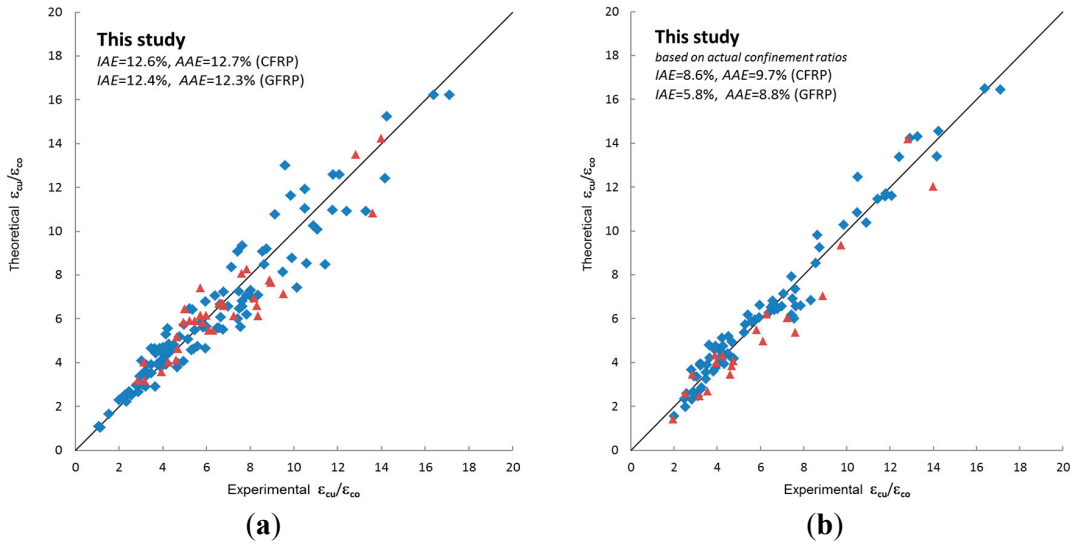

Figure 4. The assessment performance of proposed strain models for (**a**) predicted confinement ratio f_l/f_{co} based on ultimate fiber strain ε_{fu} from Model Ib, II, III, V,VI; (**b**) actual confinement ratio $f_{l,a}/f_{co}$ based on $\varepsilon_{h,u}$ from Model IV and VII, ♦ for CFRP sheets, ▲ for GFRP sheets.

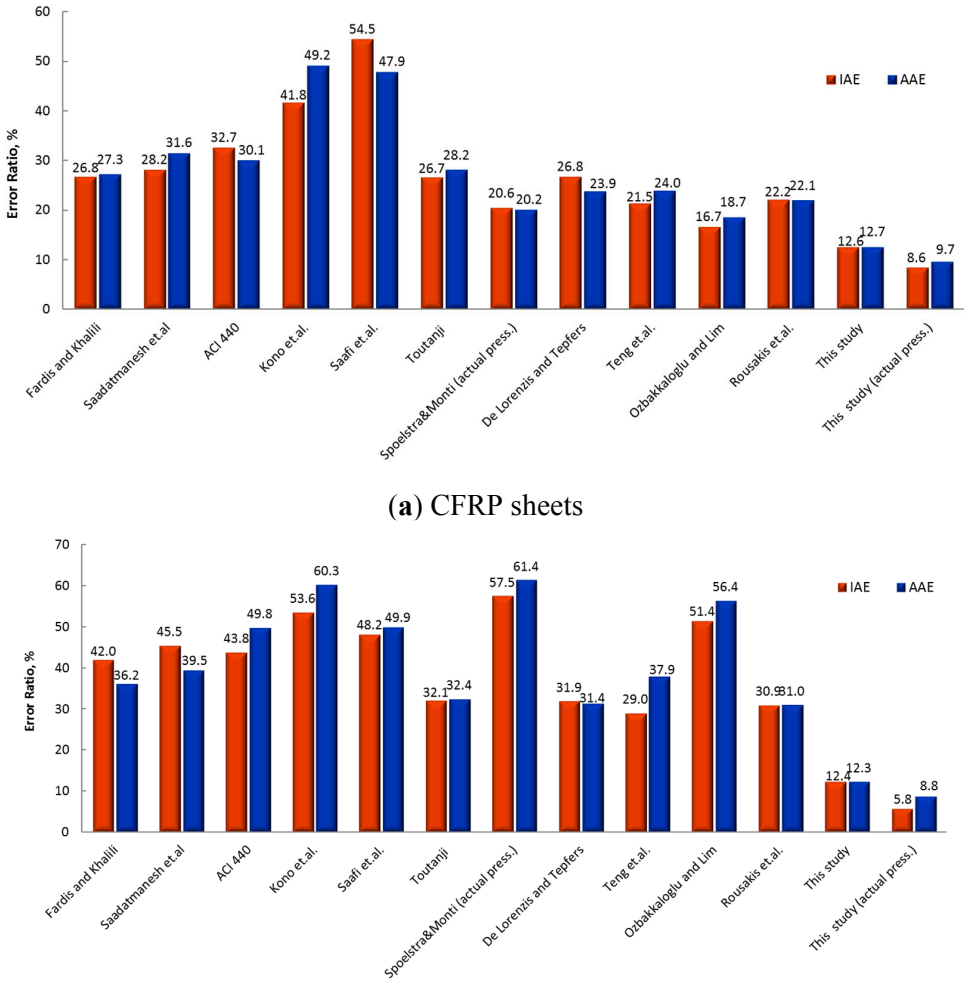

Figure 5. Error ratios of all the models under consideration for (**a**) CFRP sheets and (**b**) CFRP sheets.

4. Conclusions

In this study, a design oriented combined model was developed to predict the ultimate strengths and ultimate strains in an extensive range of unconfined strength (7 to 190 MPa) for FRP-wrapped circular columns. The following results are drawn from this study:

(1) Modified Hoek–Brown strength criterion was revisited and the range of unconfined strength was extended to f_{co} = 114 MPa.

(2) An empirical strength model with high precision was presented by encompassing UHSC and UHPC from f_{co} = 108 to 190 MPa.

(3) Strain models were developed and expressed for CFRP, GFRP from f_{co} = 15 to 170 MPa. It is realized that, when these models were compared with existing ones in the current literature, IAE and AAE ratios of produced strain models are very satisfactory.

(4) To evaluate the models, Integral Absolute Error (IAE) may be more sensitive than the Average Absolute Error (AAE) commonly used in the literature.

(5) This design-oriented combined model can be effectively used for predesign purposes or fast checks of solutions.

(6) Since the experimental strain data for GFRP sheets are relatively limited in the literature, the relevant model may be revisited in the future.

Author Contributions: Konuralp Girgin investigated and processed strain data; Zehra Canan Girgin investigated new strength data and carried out regression analyses and evaluated by graphics for strength and strain data; Zehra Canan Girgin and Konuralp Girgin discussed the results and prepared the manuscript.

Conflicts of Interests: The authors declare no conflict of interest.

References

1. Samaan, M.; Mirmiran, A.; Shahawy, M. Modeling of concrete confined by fiber composites. *J. Struct. Eng.* **1998**, *124*, 1025–1031. [CrossRef]
2. Fardis, M.N.; Khalili, H. Concrete encased in fiberglass-reinforced plastic. *ACI Struct. J.* **1981**, *78*, 440–445.
3. Huang, L.; Sun, X.; Yan, L.; Zhu, D. Compressive behavior of concrete confined with GFRP tubes and steel spirals. *Polymers* **2015**, *7*, 851–875. [CrossRef]
4. Howie, I.; Karbhari, V.M. Effect of Materials Architecture on Strengthening Efficiency of Composite Wraps for Deteriorating Columns in the North-East. In *Infrastructure: New Materials and Methods of Repair*; Basham, K.D., Ed.; American Society of Civil Engineers: New York, NY, USA, 1994; pp. 199–206.
5. Karbhari, V.M.; Gao, Y. Composite jacketed concrete under uniaxial compression-verification of simple design equations. *J. Mater. Civ. Eng.* **1997**, *9*, 185–193. [CrossRef]
6. Watanabe, K.; Nakamura, H.; Honda, T.; Toyoshima, M.; Iso, M.; Fujimaki, T.; Kaneto, M.; Shirai, N. Confinement Effect of FRP Sheet on Strength and Ductility of Concrete Cylinders under Uniaxial Compression. In Proceedings of the 3rd International Symposium on Non-Metallic (FRP) Reinforcement for Concrete Structure, Sapporo, Japan, 14–16 October 1997; pp. 233–240.
7. Rousakis, T. *Experimental Investigation of Concrete Cylinders Confined by Carbon FRP Sheets, under Monotonic and Cyclic Axial Compressive Load*; Chalmers University of Technology: Göteborg, Sweden, 2001; p. 87.
8. Ilki, A.; Peker, O.; Karamuk, E.; Demir, C.; Kumbasar, N. FRP retrofit of low and medium strength circular and rectangular reinforced concrete columns. *J. Mater. Civ. Eng.* **2008**, *20*, 169–188. [CrossRef]
9. Cui, C.; Sheikh, S.A. Experimental study of normal- and high-strength concrete confined with fiber-reinforced polymers. *J. Compos. Constr.* **2010**, *14*, 553–561. [CrossRef]
10. Song, X.; Gu, X.; Li, Y.; Chen, T.; Zhang, W. Mechanical behavior of FRP-strengthened concrete columns subjected to concentric and eccentric compression loading. *J. Compos. Constr.* **2013**, *17*, 336–346. [CrossRef]
11. Rochette, P.; Labossière, P. Axial testing of rectangular column models confined with composites. *J. Compos. Constr.* **2000**, *4*, 129–136. [CrossRef]
12. Dai, J.G.; Bai, Y.L.; Teng, J.G. Behaviour and modeling of concrete confined with FRP composites of large deformability. *J. Compos. Constr.* **2011**, *15*, 963–973. [CrossRef]
13. Campione, G.; La Mendola, L.; Monaco, A.; Valenza, A.; Fiore, V. Behavior in compression of concrete cylinders externally wrapped with basalt fibers. *Compos. Part B* **2015**, *69*, 576–586. [CrossRef]
14. Bai, Y.L.; Dai, J.G.; Teng, J.G. Cyclic compressive behavior of concrete confined with large rupture strain FRP composites. *J. Compos. Constr.* **2014**, *18*, 04013025. [CrossRef]
15. Ispir, M. Monotonic and cyclic compression tests on concrete confined with PET-FRP. *J. Compos. Constr.* **2014**, *19*, 04014034. [CrossRef]
16. Yan, L. Plain concrete cylinders and beams externally strengthened with natural flax fabric reinforced epoxy composites. *Mater. Struct.* **2015**. [CrossRef]
17. Rousakis, T. Hybrid confinement of concrete by FRP sheets and fiber ropes under cyclic axial compressive loading. *J. Compos. Constr.* **2013**, *17*, 732–743. [CrossRef]
18. Rousakis, T.C.; Tourtouras, I.S. RC columns of square section-passive and active confinement with composite ropes. *Compos. Part B* **2014**, *58*, 573–581. [CrossRef]
19. Feng, P.; Cheng, S.; Bai, Y.; Ye, L. Mechanical behavior of concrete-filled square steel tube with FRP-confined concrete core subjected to axial compression. *Compos. Struct.* **2015**, *123*, 312–324. [CrossRef]
20. Vincent, T.; Ozbakkaloglu, T. Compressive behavior of prestressed high-strength concrete-filled aramid FRP tube columns: Experimental observations. *J. Compos. Constr.* **2015**. [CrossRef]
21. Pon, T.H.; Li, Y.F.; Shih, B.J.; Han, M.S.; Chu, G.D.; Chiu, Y.J. Experiments of Scale Effects on the Strength of FRP Reinforced Concrete. In Proceedings of the 4th National Conference on Structural Engineering, Taipei, China, September 1998; pp. 2133–2140.

22. Miyauchi, K.; Inoue, S.; Kuroda, T.; Kobayashi, A. Strengthening effects of concrete columns with carbon fiber sheet. *Trans. Jpn. Concr. Inst.* **1999**, *21*, 143–150.
23. Berthet, J.F.; Ferrier, E.; Hamelin, P. Compressive behavior of concrete externally confined by composite jackets. Part A: Experimental study. *Constr. Build. Mater.* **2005**, *19*, 223–232. [CrossRef]
24. Ozbakkaloglu, T.; Vincent, T. Axial compressive behavior of circular high-strength concrete-filled FRP tubes. *J. Compos. Constr.* **2013**, *18*, 1–11. [CrossRef]
25. Zohrevand, P.; Mirmiran, A. Behavior of ultra high-performance concrete confined by fiber-reinforced polymers. *J. Mater. Civ. Eng.* **2011**, *23*, 1727–1734. [CrossRef]
26. Guler, S.; Copur, A.; Aydogan, M. Nonlinear finite element modeling of FRP-wrapped UHPC columns. *Comput. Concr.* **2013**, *12*, 413–429. [CrossRef]
27. Hoek, E.; Kaiser, P.K.; Bawden, W.F. *Support of Underground Excavations in Hard Rock*; Balkema, A.A., Ed.; CRC Press: Rotterdam, The Netherlands, 1995; p. 215.
28. Girgin, Z.C.; Arıoglu, N.; Arıoglu, E. Evaluation of strength criteria for very-high-strength concretes under triaxial compression. *ACI Struct. J.* **2007**, *104*, 278–284.
29. Girgin, Z.C. A modified failure criterion to predict ultimate strength of circular columns confined by different materials. *ACI Struct. J.* **2009**, *106*, 800–809.
30. Lam, L.; Teng, J.G. Design-oriented stress-strain model for FRP-confined concrete. *Constr. Build. Mater.* **2003**, *17*, 471–489. [CrossRef]
31. Benzaid, R.; Mesbah, H.; Chikh, N. FRP-confined concrete cylinders: Axial compression experiments and strength model. *J. Reinf. Plast. Compos.* **2010**, *29*, 2469–2488. [CrossRef]
32. Ozbakkaloglu, T.; Lim, J.C. Axial compressive behavior of FRP-confined concrete: Experimental test database and a new design-oriented model. *Compos. Part B* **2013**, *55*, 607–634. [CrossRef]
33. Spoelstra, M.R.; Monti, G. FRP-confined concrete model. *J. Compos. Constr.* **1999**, *3*, 143–150. [CrossRef]
34. Pessiki, S.; Harries, K.A.; Kestner, J.; Sause, R.; Ricles, J.M. The axial behavior of concrete confined with fiber reinforced composite jackets. *J. Compos. Constr.* **2001**, *5*, 237–245. [CrossRef]
35. Vincent, T.; Ozbakkaloglu, T. Influence of concrete strength and confinement method on axial compressive behavior of FRP confined high- and ultra-high-strength concrete. *Compos. Part B* **2013**, *50*, 413–428. [CrossRef]
36. Richart, E.; Brandtzaeg, A.; Brown, R.L. *Failure of Plain and Spirally Reinforced Concrete in Compression*; University of Illinois, Engineering Experimental Station: Champaign, IL, USA, 1929; Volume 190.
37. Mander, J.B.; Priestley, J.N.; Park, R. Theoretical stress-strain model for confined concrete. *J. Struct. Eng.* **1988**, *114*, 1804–1826. [CrossRef]
38. Saadatmanesh, H.; Ehsani, M.R.; Li, M.W. Strength and ductility of concrete columns externally reinforced with fiber composite straps. *ACI Struct. J.* **1994**, *91*, 434–447.
39. *Guide for the Design and Construction of Externally Bonded FRP Systems for Strengthening Concrete Structures*; ACI 440.2R-08; American Concrete Institute (ACI) Committee: Farmington Hills, MI, USA, 2008.
40. Kono, S.; Inazuni, M.; Kaku, T. Evaluation of Confining Effects of CFRP Sheets on Reinforced Concrete Members. In Proceedings of the 2nd International Conference on Composites in Infrastructure, Tucson, AZ, USA, 5–7 January 1998.
41. Saafi, M.; Toutanji, H.A.; Li, Z. Behaviour of concrete columns confined with fiber reinforced polymer tubes. *ACI Mater. J.* **1999**, *96*, 500–509.
42. Xiao, Y.; Wu, H. Compressive behavior of concrete confined by carbon fiber composite jackets. *J. Mater. Civ. Eng.* **2000**, *12*, 139–146. [CrossRef]
43. Toutanji, H.A. Stress-strain characteristics of concrete columns externally confined with advanced fibre composite sheets. *ACI Mater. J.* **1999**, *96*, 397–402.
44. Teng, J.; Jiang, T.; Lam, L.; Luo, Y. Refinement of a design-oriented stress–strain model for FRP-confined concrete. *J. Compos. Constr.* **2009**, *13*, 269–278. [CrossRef]
45. Rousakis, T.C.; Rakitzis, T.D.; Karabinis, A.I. Design-oriented strength model for FRP-confined concrete members. *J. Compos. Constr.* **2012**, *16*, 615–625. [CrossRef]
46. Rousakis, T.; Rakitzis, T.; Karabinis, A. Empirical Modelling of Failure Strains of Uniformly FRP Confined Concrete Columns. In Proceedings of the 6th International Conference on FRP Composites in Civil Engineering (CICE), Rome, Italy, 13–15 June 2012.

47. Johnston, I.W. Comparison of two strength crieria for intact rock. *J. Geotech. Eng. Div.* **1985**, *111*, 1449–1454. [CrossRef]
48. Girgin, Z.C. Modified Johnston failure criterion from rock mechanics to predict the ultimate strength of fiber reinforced polymer (FRP) confined columns. *Polymers* **2014**, *6*, 59–75. [CrossRef]
49. Mirmiran, A.; Shahawy, M. Behavior of concrete columns confined by fiber composites. *J. Struct. Eng.* **1997**, *123*, 583–590. [CrossRef]
50. Thériault, M.; Neale, K.W. Design equations for axially loaded reinforced concrete columns strengthened with FRP wraps. *Can. J. Civ. Eng.* **2000**, *27*, 1011–1020. [CrossRef]
51. Karabinis, A.I.; Rousakis, T.C. Concrete confined by FRP material: A plasticity approach. *Eng. Struct.* **2002**, *24*, 923–932. [CrossRef]
52. Lin, C.; Li, Y. An effective peak stress formula for concrete confined with carbon fibre reinforced plastics. *Can. J. Civ. Eng.* **2003**, *30*, 882–889. [CrossRef]
53. Lin, H.L.; Liao, C.I. Compressive strength of reinforced concrete-column confined by composite materials. *Compos. Struct.* **2004**, *65*, 239–250. [CrossRef]
54. Thériault, M.; Neale, K.W.; Claude, S. Fiber-reinforced polymer-confined circular concrete columns: Investigation of size and slenderness effects. *J. Compos. Constr.* **2004**, *8*, 323–331. [CrossRef]
55. Lam, L.; Teng, J.G. Ultimate condition of FRP-confined concrete. *J. Compos. Constr.* **2004**, *8*, 539–548. [CrossRef]
56. El Chabib, H.; Nehdi, M.; El Naggar, M.H. Behavior of SCC confined in short GFRP tubes. *Cem. Concr. Compos.* **2005**, *27*, 55–64. [CrossRef]
57. Mandal, S.; Hoskin, A.; Fam, A. Influence of concrete strength on confinement effectiveness of fiber-reinforced polymer circular jackets. *ACI Struct. J.* **2005**, *102*, 383–392.
58. Triantafillou, T.C.; Papanicolaou, C.G.; Zissimopoulos, P.; Laourdekis, T. Concrete confinement with textile-reinforced mortar jackets. *ACI Struct. J.* **2006**, *103*, 28–37.
59. Almussalam, T.H. Behavior of normal and high-strength concrete cylinders confined with E-glass/epoxy composite laminates. *Compos. Part B* **2007**, *38*, 629–639. [CrossRef]
60. Jiang, T.; Teng, J.G. Analysis-oriented stress-strain models for FRP-confined concrete. *Eng. Struct.* **2007**, *29*, 2968–2986. [CrossRef]
61. Wang, L.M.; Wu, Y.F. Effect of corner radius on the performance of CFRP-confined square concrete columns: Test. *Eng. Struct.* **2008**, *30*, 493–505. [CrossRef]
62. Harries, K.A.; Kharel, G. Behavior and modeling of concrete subject to variable confining pressure. *ACI Mater. J.* **2002**, *99*, 180–189.
63. Youssef, M.N.; Feng, M.Q.; Mosallam, A.S. Stress–strain model for concrete confined by FRP composites. *Compos. B Eng.* **2007**, *38*, 614–628. [CrossRef]
64. Chikh, N.; Benzaid, R.; Mesbah, H. An experimental investigation of circular RC columns with various slenderness confined with CFRP sheets. *Arab J. Sci. Eng.* **2012**, *37*, 315–323. [CrossRef]
65. *Building Code Requirements for Structural Concrete (ACI Committee 318) and Commentary*; American Concrete Institute Committee: Farmington Hills, MI, USA, 2008; p. 520.
66. *Report on High-Strength Concrete*; ACI 363R-10; American Concrete Institute Committee: Farmington Hills, MI, USA, 2010; p. 65.
67. Ahmad, S.M.; Shah, S.P. Stress-strain curves of concrete confined by spiral reinforcement. *ACI J. Proc.* **1982**, *79*, 484–490.
68. Mesbah, H.A.; Lachemi, M.; Aïtcin, P.C. Determination of elastic properties of high-performance concrete at early ages. *ACI Mater. J.* **2002**, *99*, 37–41.
69. Noguchi, T.; Tomosawa, F.; Nemati, K.M.; Chiaia, B.M.; Fantilli, A.P. A practical equation for elastic modulus of concrete. *ACI Struct. J.* **2009**, *106*, 690–696.
70. *Fib Model Code for Concrete Structures (fib MC2010)*; Ernst & Sohn Publishing: Lausanne, Switzerland, 2013; p. 434.
71. Magureanu, C.; Sosa, I.; Negrutiu, C.; Heghes, B. Mechanical properties and durability of ultra-high performance concrete. *ACI Mater. J.* **2012**, *109*, 177–184.
72. *Designers' Guide to EN1994-1-1. Eurocode 4: Design of composite steel and concrete structures. Part 1.1: General Rules and Rules for Buildings*; British Standards Institution: London, UK, 2004.

73. De Lorenzis, L.; Tepfers, R. Comparative study of models on confinement of concrete cylinders with fiber-reinforced polymer composites. *J. Compos. Constr.* **2003**, *7*, 219–237. [CrossRef]
74. Girgin, Z.C. (Yildiz Technical University, Istanbul, Turkey); Monti, G. (Sapienza University of Rome, Rome, Italy). Personal communication, 2015.
75. Nisticò, N.; Pallini, F.; Rousakis, T.; Wu, Y.F.; Karabinis, A. Peak strength and ultimate strain prediction for FRP confined square and circular concrete sections. *Compos. Part B* **2014**, *67*, 543–554. [CrossRef]